SUPPLEMENTAL FIGURES LEGEND

Fig S1: Biological replicates. A) Correlation of biological replicates. Scatter plots depicting the correlation between normalized methylation values of two biological replicates for each cell line. **B) methylation in *HOXA* cluster of biological replicates.** Shown are the methylation profiles at the *HOXA* cluster for individual arrays. For forming the averaged profile, the Fib._2 and Cres2_2 arrays were not used. For DMR screening we used all data as is.

Fig S2: Differential methylation distributions. A) The distribution of the difference in methylation between ORMES-22 and fibroblasts in hyper-DMRs **B)** The distribution of the difference in methylation between ORMES-22 and fibroblasts in hypo-DMRs**.**

Fig S3: Sequence analysis of hypo- and hyper- DMRs at low CpG levels. A) dinucleotide distribution. The frequency of dinucleotides was computed for hypo-DMRs (green), hyper-DMRs (red) and background regions (grey) with average CpG content less than 15. Background regions were chosen as regions in which the difference between ORMES-22, fibroblasts and CRES-2 was insignificant (KS p-value>0.001). **B) CpG sequence context.** Shown are the frequency profiles for dinucleotides following a CpG in hypo-DMRs (green), hyper-DMRs (red) and background regions (grey) in which the average CpG content is less than 15.

Fig S4: Sequence analysis of hypo- and hyper- DMRs at intermediate CpG levels. A) dinucleotiide distribution. B) CpG sequence context. As Fig S3, for average CpG content between 15 and 40.

Fig S5: DMRs at regulated promoters. Induced and repressed genes (here at least two fold) were extracted using gene expression array profiles on fibroblasts, ORMES-22 and CRES-2. Individual tiling array probes were classified as hyper-methylated and hypo-methylated according to their fibroblast and ORMES-22 array values (normalized array difference > 0.6), and were further partitioned according to their CpG content (low: CpG < 15, intermediate: 15 < CpG < 50, high CpG > 50). We computed the number of probes at each distance relative to induced (upper) and repressed (lower) TSSs. The $\log_2$ of the ratio between this number and the number expected by chance (assuming hyper- and hypo- methylated probes are randomly

distributed) is plotted. As expected from the general anti-correlation between gene expression and DNA methylation, induced genes are enriched with hypo-methylated probes and anti-enriched for hyper-methylated probes, while repressed genes are enriched with hyper-methylated probes.

Fig S6: Occupancy of pluripotency factors. A) Oct4 occupancy. Shown are box plots for average human Oct4 occupancy on mapped monkey DMRs and background regions. We plot separately groups of regions with different levels of CpG content, dissected into groups of hyper-DMRs (red), hypo-DMRs (green), regions with low ES methylation (blue) and regions with high ES methylation (yellow). **B) Nanog occupancy**. As part A, for Nanog.

Fig S7: **Properties of low reprogramming ratio DMRs**. **A) Reprogrammed DMR size distribution.** Shown is the log size distribution of genomic intervals determined to be hypo-DMRs with reprogramming ratio less than 0.25 (limited, blue), and hypo-DMRs with reprogramming ratio greater than 0.5 (extensive, black). **B) Reprogrammed DMR CpG content**. The average number of CpGs in 500 bp windows was computed for each DMR (each CpG was counted twice) and the distribution of CpG content for limited-reprogramming hypo-DMRs and extensive-reprogramming hypo-DMRs was plotted. **C) Reprogrammed DMRs Suz12 occupancy**. Shown is the distribution of Suz12 occupancy in human ESCs on mapped monkey hypo-DMRs with limited reprogramming (blue) and in hypo-DMRs with extensive reprogramming (black). **D) Reprogrammed DMR CTCF occupancy**. Shown is the distribution of CTCF occupancy in human fibroblasts on mapped monkey hypo-DMRs with limited reprogramming (blue) and in hypo-DMRs with extensive reprogramming (black). **E) Reprogrammed DMR telomere distance distribution**. The distance from telomere was computed for each DMR and the distributions of telomere distance of limited reprogrammed hypo-DMRs and extensively reprogrammed hypo-DMRs were plotted.

Fig S8: CpG content vs. array binding ratio for all MeDIP samples. Shown are the means of MeDIP binding ratios for every biological replicate and cell line, computed for bins of weighted probes' CpG contents, (hyb_e curves, see Methods, Gal-Yam, Egger et al. 2008) and different G and C contents.

Fig S9: qPCR validation. Q-PCR amplification of genomic DNA fragments was purified by pull-down with anti-5 methylcytosine antibody. Paternally methylated *H19*

and maternally methylated *SNRPN* promoters were used as control genes. Enrichment of *H19* (black column*)* and *SNRPN* (blue column*)* was observed in IVF-derived ES cells, SCNT-derived ES cells and donor fibroblasts, consistent with CpG methylation on both the paternal and maternal alleles in these XY cells. As expected, enrichment of *H19* was observed in sperm and enrichment of *SNRPN* was observed in homozygous parthenogenetic ES cells. Enrichment values were plotted after normalization with 10% input DNA. Data represents the mean ± S.E.M. (n = 4).

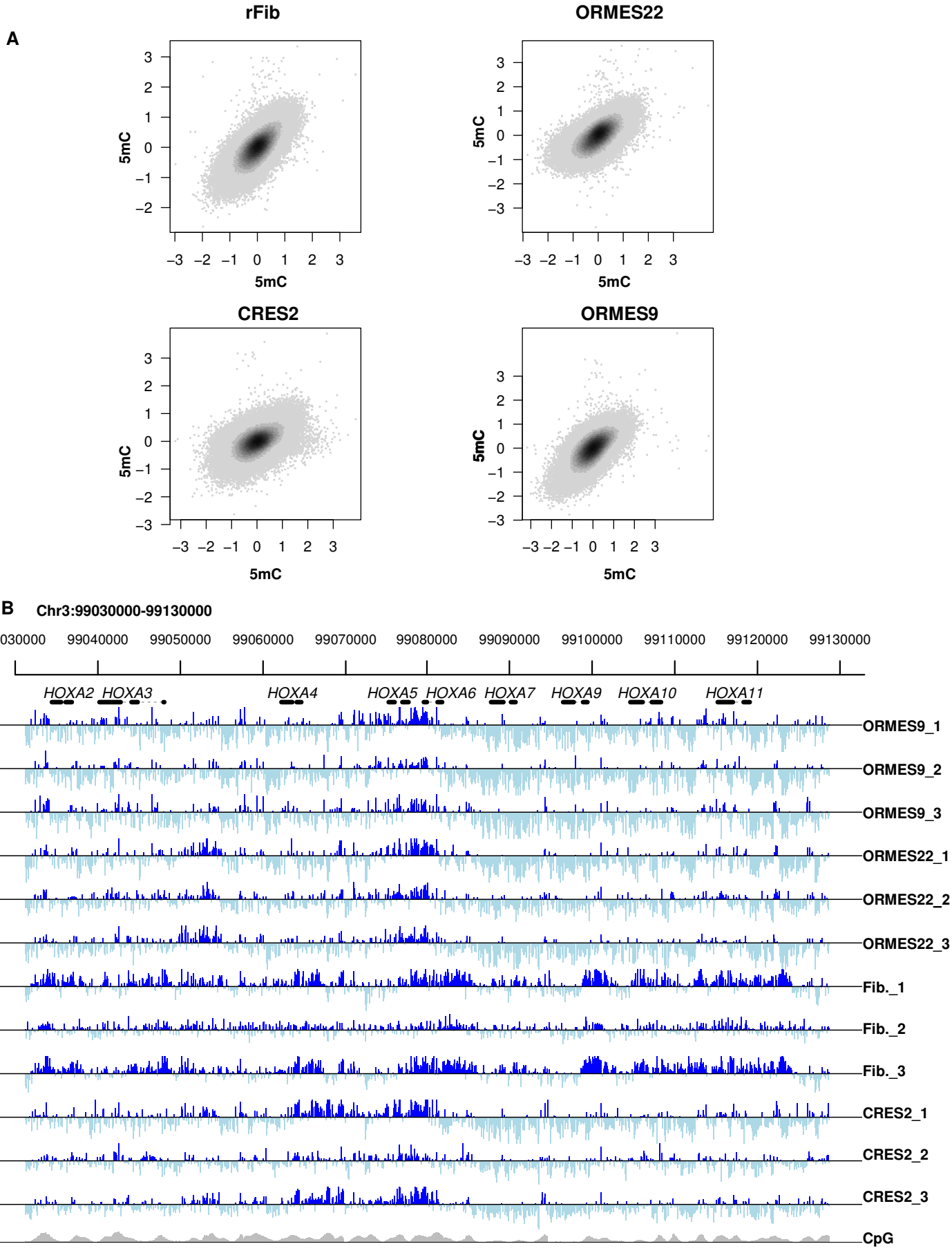
A
rFib
ORMES22
CRES2
ORMES9
5mC
B
Chr3:99030000-99130000
99030000
99040000
99050000
99060000
99070000
99080000
99090000
99100000
99110000
99120000
99130000
HOXA2
HOXA3
HOXA4
HOXA5
HOXA6
HOXA7
HOXA9
HOXA10
HOXA11
ORMES9_1
ORMES9_2
ORMES9_3
ORMES22_1
ORMES22_2
ORMES22_3
Fib._1
Fib._2
Fib._3
CRES2_1
CRES2_2
CRES2_3
CpG

Figure S1

A

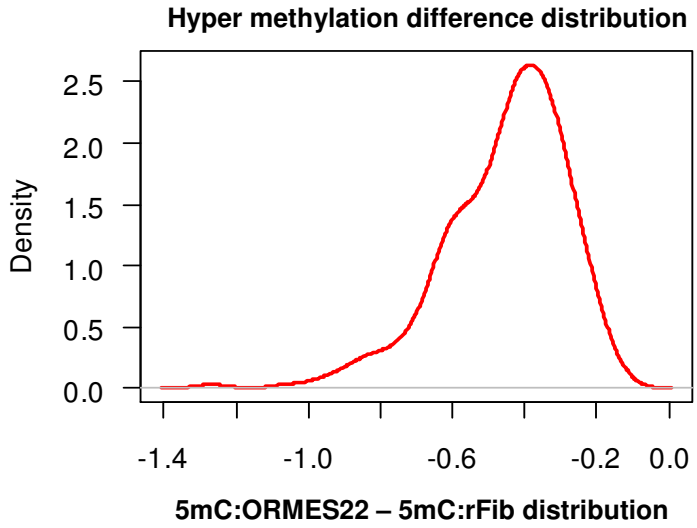
Hyper methylation difference distribution
Density
2.5
2.0
1.5
1.0
0.5
0.0
-1.4
-1.0
-0.6
-0.2
0.0
5mC:ORMES22 – 5mC:rFib distribution

B

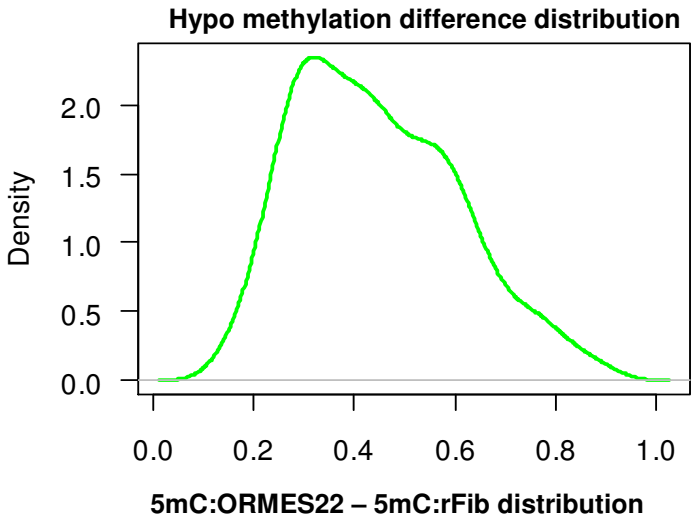
Hypo methylation difference distribution
Density
2.0
1.5
1.0
0.5
0.0
0.0
0.2
0.4
0.6
0.8
1.0
5mC:ORMES22 – 5mC:rFib distribution

Figure S2

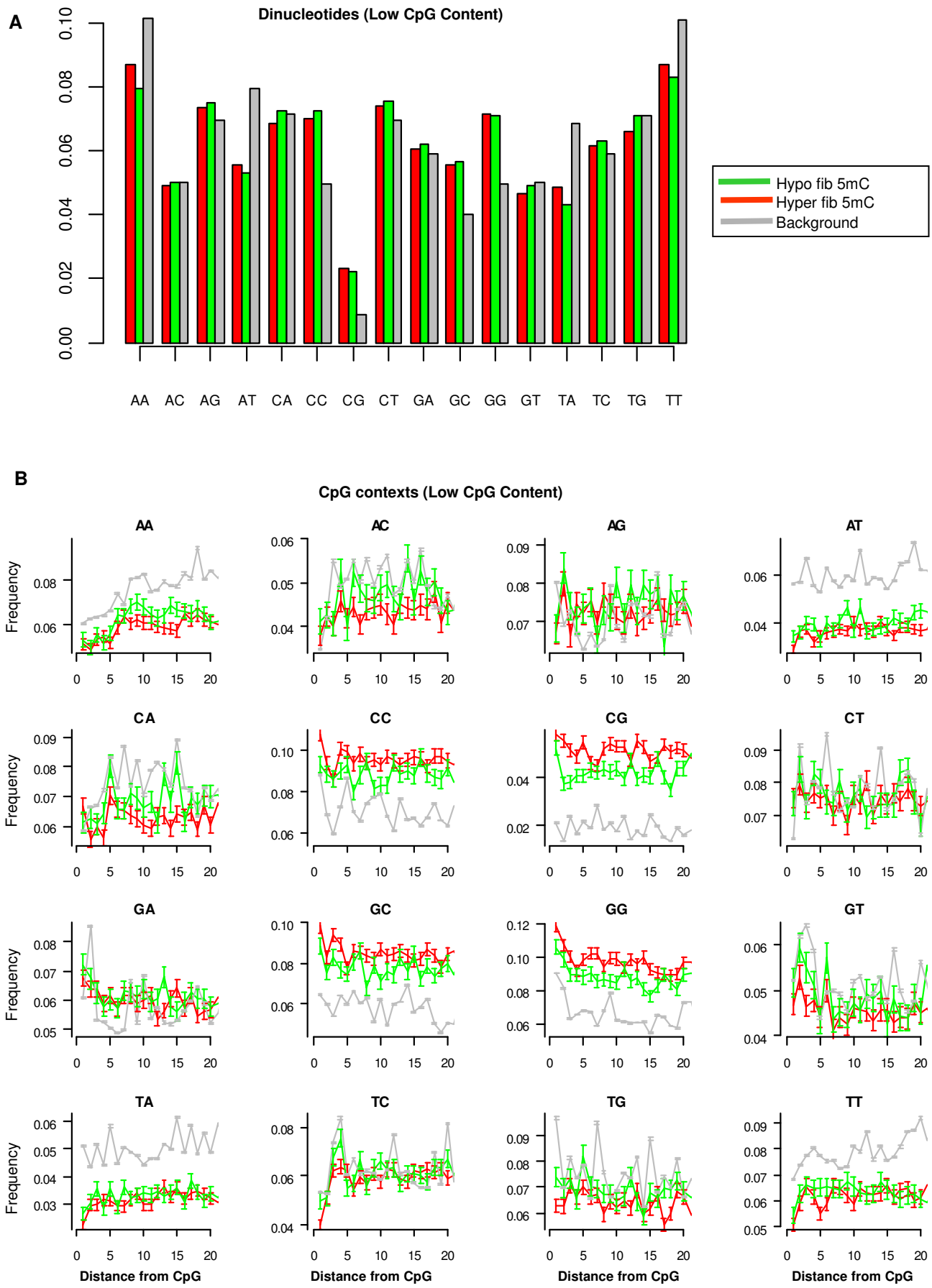
A
Dinucleotides (Low CpG Content)
0.00
0.02
0.04
0.06
0.08
0.10
AA AC AG AT CA CC CG CT GA GC GG GT TA TC TG TT
Hypo fib 5mC
Hyper fib 5mC
Background
B
CpG contexts (Low CpG Content)
AA
AC
AG
AT
CA
CC
CG
CT
GA
GC
GG
GT
TA
TC
TG
TT
Frequency
Distance from CpG

Figure S3

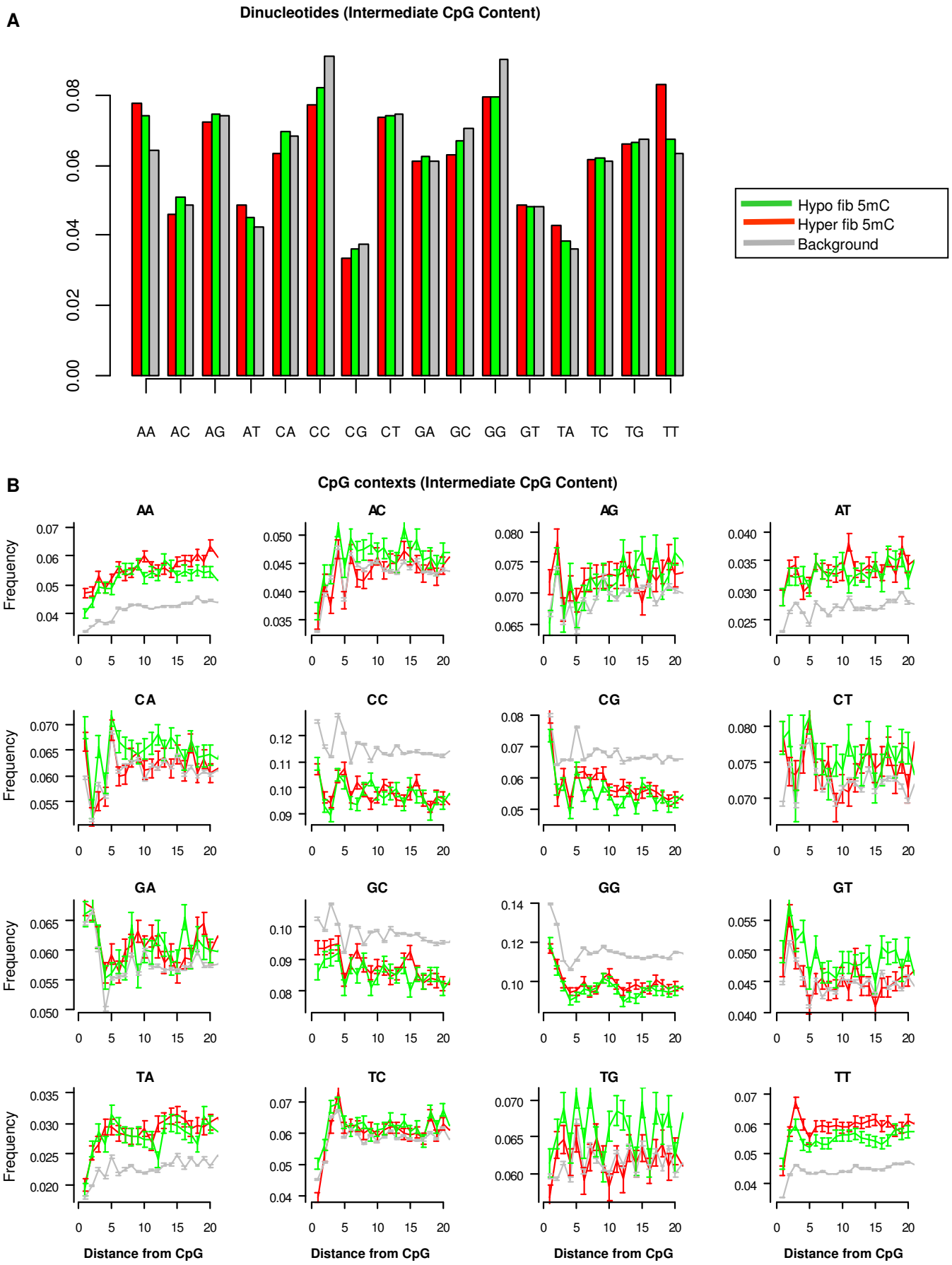
A
Dinucleotides (Intermediate CpG Content)
0.00
0.02
0.04
0.06
0.08
AA AC AG AT CA CC CG CT GA GC GG GT TA TC TG TT
Hypo fib 5mC
Hyper fib 5mC
Background
B
CpG contexts (Intermediate CpG Content)
AA
AC
AG
AT
CA
CC
CG
CT
GA
GC
GG
GT
TA
TC
TG
TT
Frequency
Distance from CpG

Figure S4

A

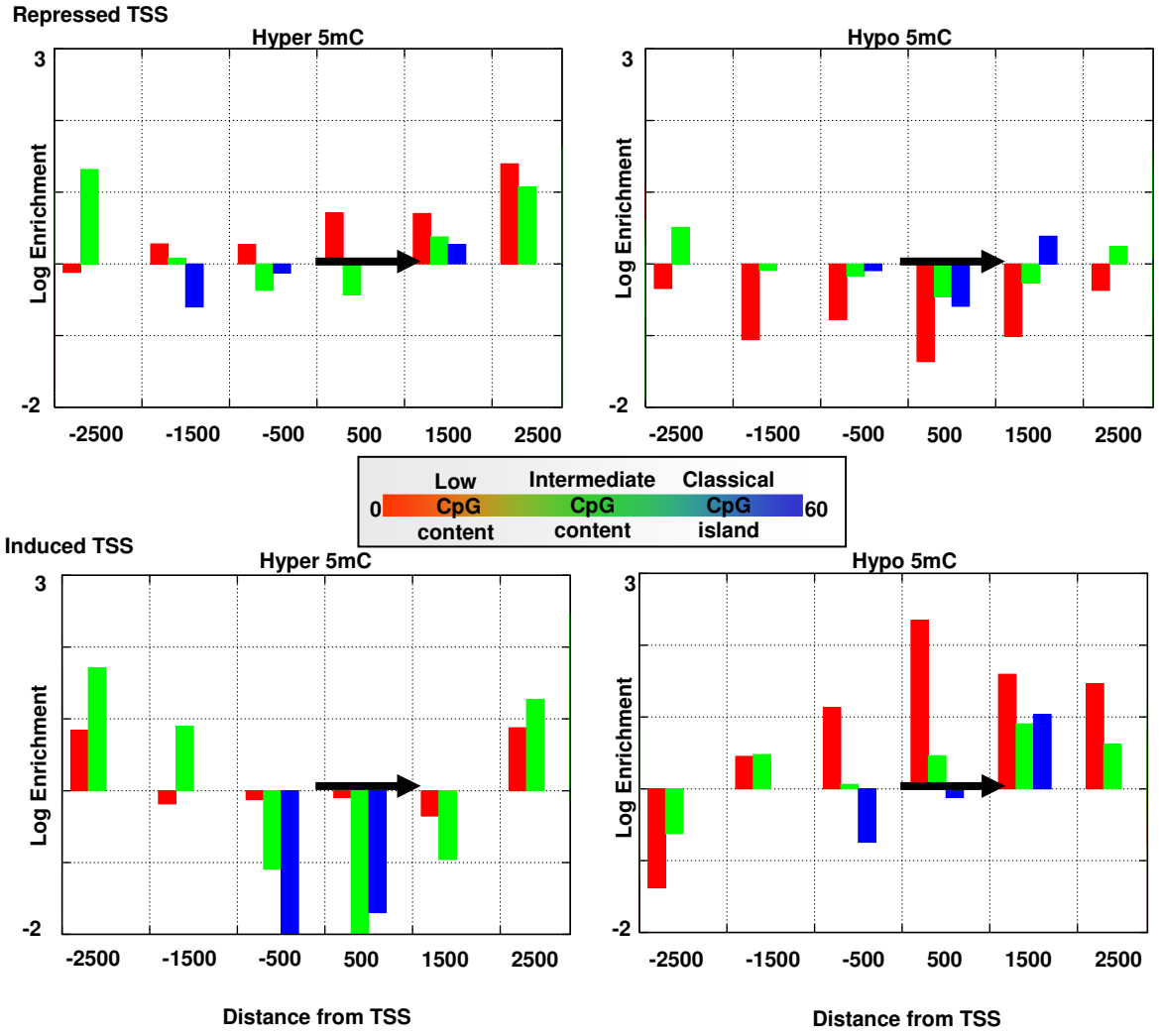
Repressed TSS
Hyper 5mC
Hypo 5mC
Log Enrichment
3
-2
-2500
-1500
-500
500
1500
2500
Low CpG content
Intermediate CpG content
Classical CpG island
0
60
Induced TSS
Hyper 5mC
Hypo 5mC
Distance from TSS
Distance from TSS

Figure S5

A

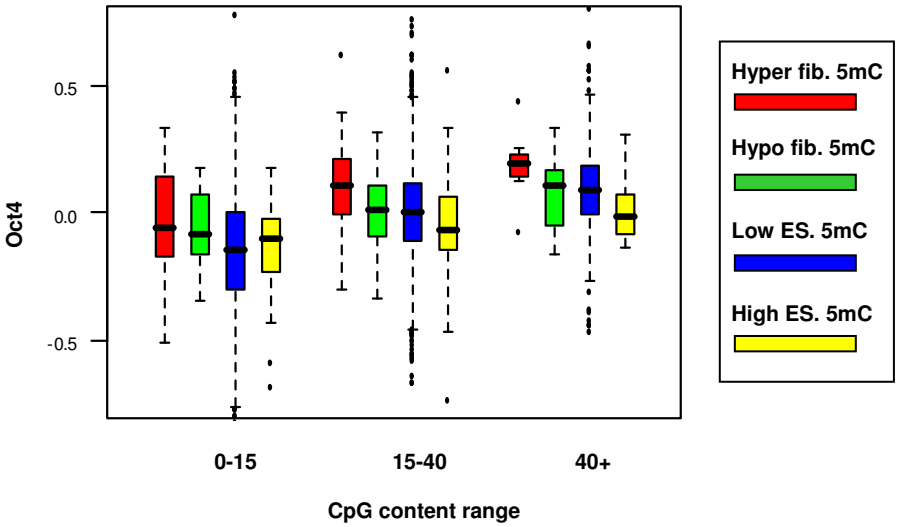
Oct4
0.5
0.0
-0.5
0-15
15-40
40+
CpG content range
Hyper fib. 5mC
Hypo fib. 5mC
Low ES. 5mC
High ES. 5mC

B

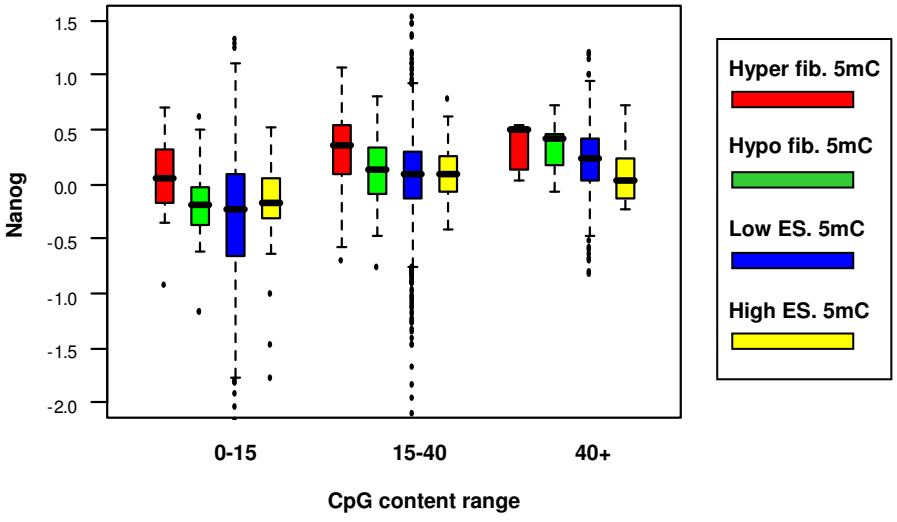
Nanog
1.5
1.0
0.5
0.0
-0.5
-1.0
-1.5
-2.0
0-15
15-40
40+
CpG content range
Hyper fib. 5mC
Hypo fib. 5mC
Low ES. 5mC
High ES. 5mC

Figure S6

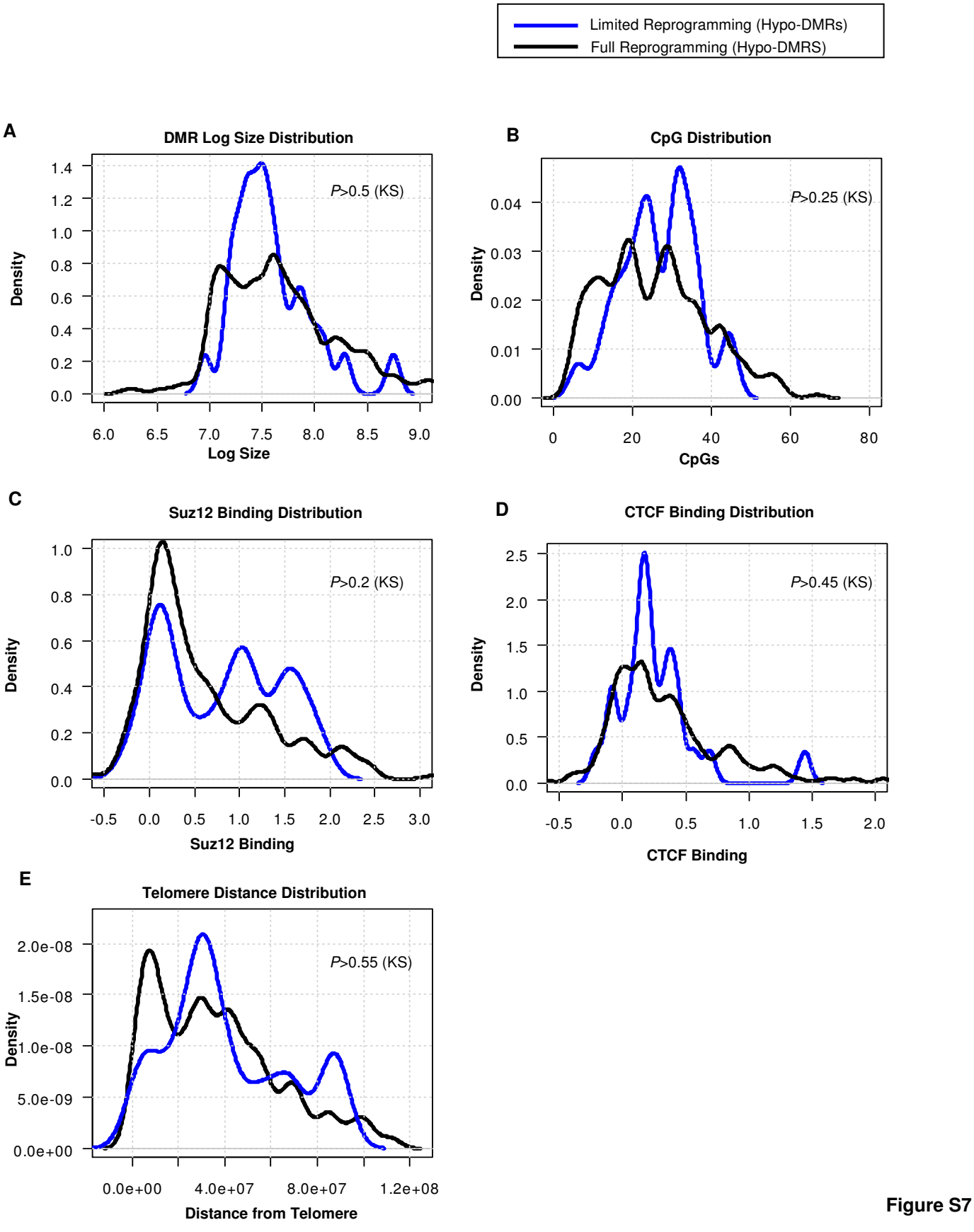
Limited Reprogramming (Hypo-DMRs)
Full Reprogramming (Hypo-DMRS)
A
DMR Log Size Distribution
P>0.5 (KS)
Density
Log Size
B
CpG Distribution
P>0.25 (KS)
Density
CpGs
C
Suz12 Binding Distribution
P>0.2 (KS)
Density
Suz12 Binding
D
CTCF Binding Distribution
P>0.45 (KS)
Density
CTCF Binding
E
Telomere Distance Distribution
P>0.55 (KS)
Density
Distance from Telomere

Figure S7

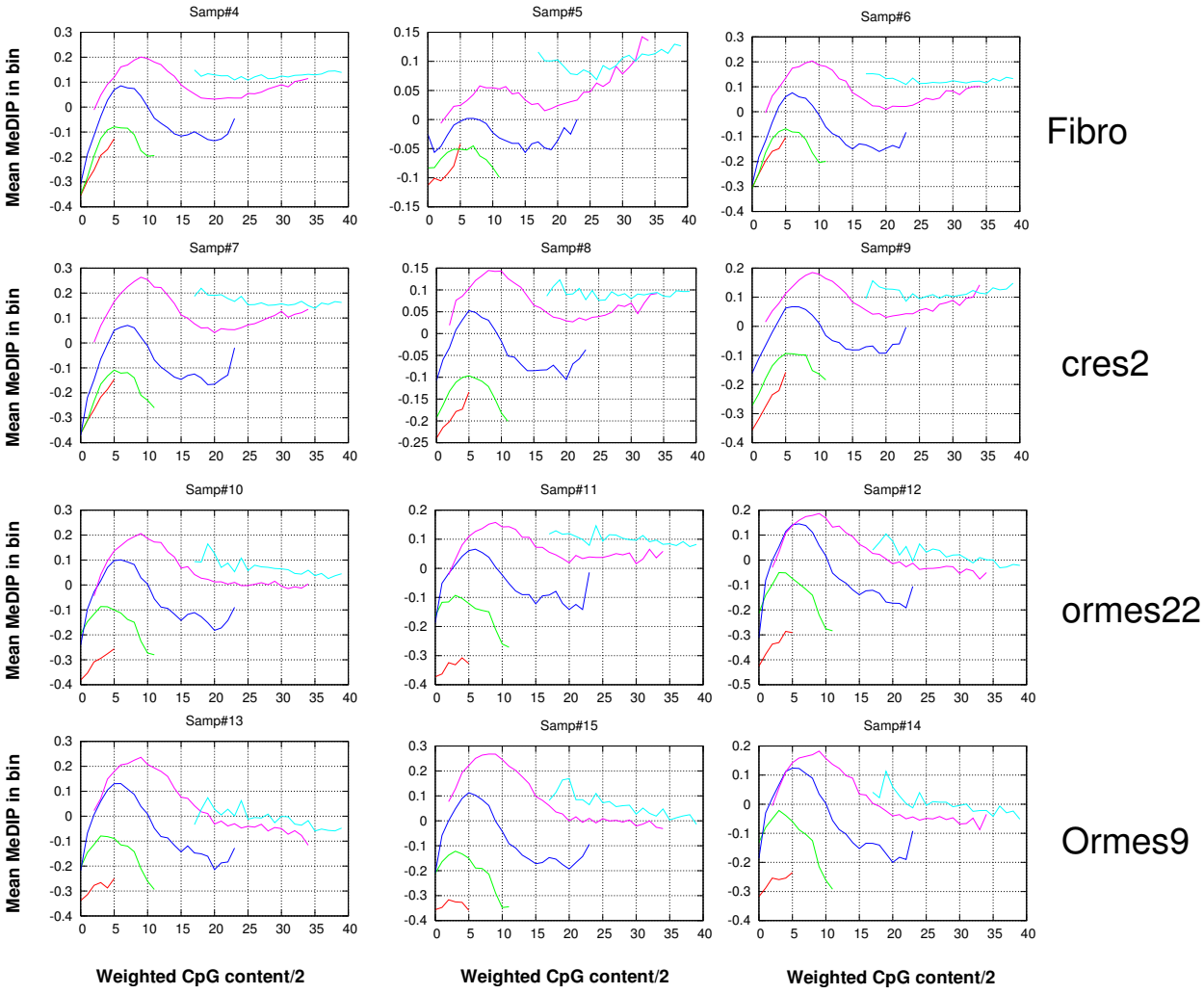
Samp#4
Samp#5
Samp#6
Samp#7
Samp#8
Samp#9
Samp#10
Samp#11
Samp#12
Samp#13
Samp#15
Samp#14
Mean MeDIP in bin
Weighted CpG content/2
Fibro
cres2
ormes22
Ormes9

Figure S8

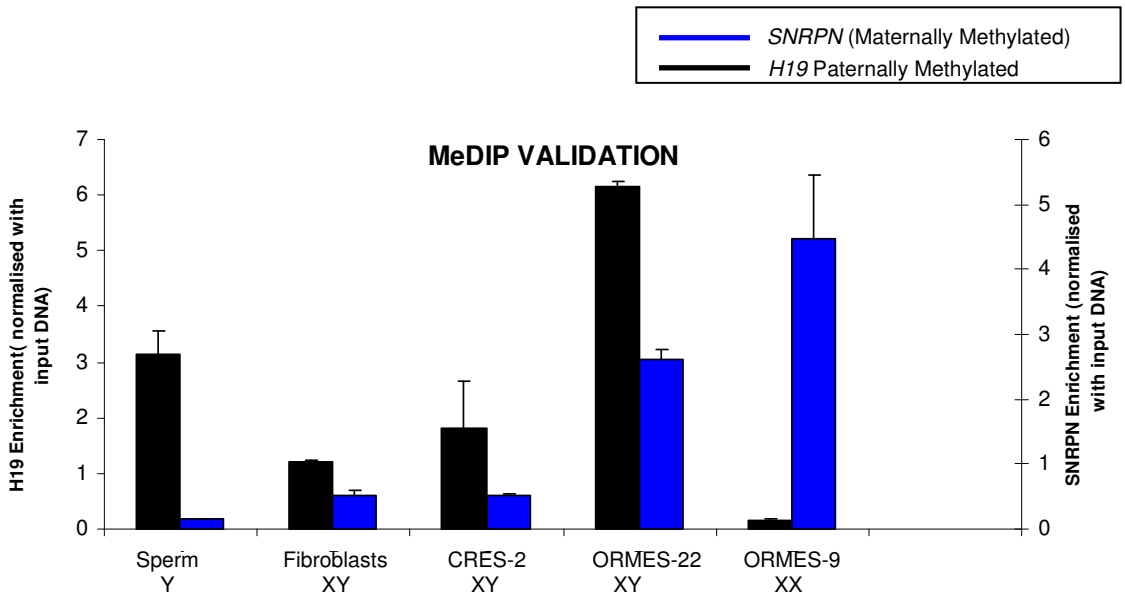
SNRPN (Maternally Methylated)
H19 Paternally Methylated
MeDIP VALIDATION
H19 Enrichment(normalised with input DNA)
SNRPN Enrichment (normalised with input DNA)
0
1
2
3
4
5
6
7
Sperm
Y
Fibroblasts
XY
CRES-2
XY
ORMES-22
XY
ORMES-9
XX

Figure S9